PHYSICAL REVIEW B

CONDENSED MATTER

THIRD SERIES, VOLUME 44, NUMBER 13 1 OCTOBER 1991-I

Melting transition and properties of the plastic crystal and fluid phases of N_2 deposited on graphite

M. Roth and R. D. Etters

Department of Physics, Colorado State University, Fort Collins, Colorado 80523

(Received 20 March 1991)

A Monte Carlo method using both constant-pressure and constant-surface-density ensembles, with free surface and deformable periodic boundary conditions is employed to examine the melting and orientational behavior of partial and complete monolayers of N_2 on graphite. A simple argument concerning the ability of these systems, or lack of it, to fluctuate and expand in the plane of the substrate is sufficient to explain the drastic change in melting temperature T_M, as the adlayer surface density is increased toward monolayer completion. The calculated average orientation of the N_2 molecules is parallel to the substrate plane at all temperatures investigated, $30 \leq T \leq 95$ K, although out-of-plane orientational fluctuations increase substantially with increasing T. The nature of the melting transition of partial and complete monolayers is discussed, and it is shown that a small 256-molecule patch with free-surface boundary conditions exhibits nearly asymptotic behavior. Various order parameters and distributions are calculated to interpret system behavior.

I. INTRODUCTION

Various experiments, including low-energy electron diffraction (LEED),[1-5] neutron diffraction,[6,7] heat capacity,[8-10] vapor-pressure measurements,[9] and calorimetric studies,[9,11,12] have provided a fairly detailed description of N_2 adsorbed on graphite at densities $\rho \leq 1$, where the upper limit refers to a complete monolayer, in units of 0.0636 molecules/Å^2. At these densities and low temperatures the N_2 molecules form a two-sublattice herringbone arrangement, and the mass centers conform to the substrate symmetry by registering into the $\sqrt{3}\times\sqrt{3}$ structure. At $T_{OD} \simeq 28$ K, an orientational order-disorder transition[2,13] occurs, above which the molecules act as weakly hindered, planar rotors with short-ranged orientation correlations that diminish with increasing temperature. The $\sqrt{3}\times\sqrt{3}$ center-of-mass structure, however, persists until melting.[6] It has also been observed[6,7] that registered islands are formed for fractional monolayer coverages, and interpretation of the data suggests that these clusters may contain as few as $10^2 \lesssim N \lesssim 10^3$ molecules.

The melting temperature has been observed[1,6,8,9] to be virtually constant at $T_M \simeq 47$ K, for all surface densities below and within a few percent of monolayer completion. However, T_M dramatically rises[8] to about 85 K as the density is further increased toward monolayer coverage, with $\rho = 1$. Interpretation of neutron diffraction[6] and heat-capacity data[8,9] has led to the claim that the low-temperature melting transition is first order with an entropy change of $\Delta S/Nk_B = 2.3 \pm 0.1$, where k_B is Boltzmann's constant, and the high-temperature transition at monolayer coverage is second order. It has been further argued[9] that the low value of T_M for partial monolayers is due to the large fraction of edge to interior molecules, where the former are expected to be more weakly bound because their bonds are not saturated.

Theoretical studies of two-dimensional melting have provided considerable insight into this transition. Kosterlitz, Thouless, Halperin, Nelson, and Young[14] (KTHNY) have constructed a general theory which is dislocation mediated and involves two second-order transitions. The first is from the solid into a hexatic phase in which the vectors connecting molecular mass centers to their nearest neighbors exhibit sixfold azimuthal symmetry. The second is from the hexatic phase into an isotropic liquid. It has been noted, however, that substrate interactions and ever-present departures of a physical layer from perfect translational symmetry could result in first-order transitions. Another complexity is that physical layers are only "quasi" two dimensional (2D), which diminishes the predictive qualities of strictly 2D models. Frenkel and McTague[15] examined a strictly 2D layer of atoms interacting via a Lennard-Jones 6–12 potential in a molecular dynamics (MD) simulation using an (N,ρ,T) ensemble, where N is the number of particles, ρ is the sur-

face density, and T is the temperature. Their results support the KTHNY theory,[14] but this has been disputed by Abraham[16] who used a (N,P,T) Monte Carlo (MC) method that indicated the melting transition is first order, replete with hysteresis. The 2D pressure is denoted by P. There continues to be controversy, but it appears that the Kosterlitz, Thouless, Feynman criterion is satisfied in Abraham's calculations.[17] There have been numerous[18–25] other calculations on strictly 2D model systems, mostly with Lennard-Jones interactions. Many report hysterisis across the melting transition, and there seems to be more evidence for first-order transitions using the (N,P,T) ensemble than for (N,ρ,T). Clearly, all features are not yet resolved.

There have been several calculations[26–28] directed specifically toward melting of N_2 on graphite and properties of the fluid phase. Joshi and Tildesley[28] used an MD simulation with 140 molecules in the MD cell. The starting configuration was a rectangular strip with molecules in the $\sqrt{3}\times\sqrt{3}$ structure and random orientations. The strip was designed so that half the cell was populated and the average density across the cell was $\rho=0.5$. Periodic boundary conditions commensurate with the $\sqrt{3}\times\sqrt{3}$ structure were imposed in one direction and free surface boundary conditions in the other direction. The N_2-N_2 interaction was a Lennard-Jones 6-12 atom-atom expression with point charges used to characterize the electric multipole interactions. A 6-12 expression was also used to characterize the interaction with the substrate, which was expressed in terms of the Fourier expansion of Steele.[29] No substrate-mediated dispersion or image charge interactions were considered. They obtained a melting temperature $T_M=39$ K but, with the anisotropic modification of the substrate interaction of Carlos and Cole,[30] $T_M\simeq 45$ K. By arbitrarily increasing a term in that expression[30] by about a factor of 2, which comes from helium scattering data, they were able to increase melting several more degrees. In the fluid there was evidence of a modulation giving rise to higher mean densities around the registry sites, the center of graphite hexagons, which disappeared somewhat above T_M.

In a recent letter[31] we postulated that the fundamental distinction between melting of partial and complete N_2 monolayers is a difference in boundary conditions. For the former there are many vacancies between islands that promote thermal fluctuations in the plane of the substrate which, in turn, facilitate self-diffusion, thermal expansion, and melting at $T_M\approx 48$ K. For the complete monolayer all lattice sites are occupied and thermal expansion in the plane is eliminated by the boundary of the experimental apparatus and/or possibly by grain boundaries. Thus, only fluctuations in the z direction, normal to the plane, can provide vacancies sufficient to initiate 2D melting. These distinctions are important because the N_2-substrate interactions are an order of magnitude stronger than the in-plane N_2-N_2 interactions. Thus, fluctuations normal to the plane are difficult to thermally induce and melting by this mechanism is impeded. A related calculation by Novaco[32] clearly shows the impact on melting by suppression of fluctuations in plane, where a specialized 2D system was edge pinned.

II. METHODS AND INTERACTIONS

The interactions between N_2 molecules are represented by our atom-atom fit to *ab initio* results of Berns and van der Avoird[33] and the Gordon-Kim electron gas results of LeSar and Gordon[34] at small separations. This expression, which includes the electric multipole interactions, has proved to be a highly accurate representation of 3D N_2 in the solid, fluid, and gaseous phases over a wide range of (T,P).[35–37] This includes the characterization of solid-solid and solid-fluid phase transitions. Moreover, it has been successfully tested in various calculations of N_2 layers on graphite,[38,39] including the orientational order-disorder transition.[39] The interaction between admolecules and the substrate is composed of several terms. The overlap and direct dispersion interaction between each nitrogen atom and the substrate carbon atoms is determined using combining rules. This expression has been represented in terms of the Fourier expansion of Steele.[29] The first term in this expansion depends only on the distance of each nitrogen atom above the substrate surface z and the much smaller second term, designated E_1, is the leading term which characterizes the lateral variations in the potential across the substrate surface. Higher-order terms are negligible. Additional terms in the N_2-substrate potential include the Coulomb interactions between charges representing the N_2 multipoles and their images, induced in the graphite substrate, and the substrate-mediated dispersion relation that depends on the graphite dielectric function and the dynamic polarizability of the N_2 admolecules. Details of all the interactions are given in Ref. 38.

To examine the melting and orientational properties of the N_2 adlayer we have employed both an (N,P,T) and (N,ρ,T) MC procedure with deformable boundary conditions. Calculations were made mostly with $N=16$ and 64 molecules, but some were conducted with $N=256$, partially to ensure that there were no significant size effects. Lattice sums were taken out to 9 Å, with continuum corrections beyond. Typically averages are determined over 2×10^4 steps, and after a few thousand are neglected to minimize initial transients. Near transitions, additional steps were often required. Each step consists of randomly moving all $5N$ molecular coordinates and the three in-plane MC cell parameters. Movements in the z direction (out of plane) are unrestricted.

Fractional monolayers are characterized in two ways. First a patch of 256 molecules, initially distributed in a nearly circular pattern with free surface boundary conditions, was investigated using an (N,P,T) ensemble. Second, a deformable MC cell containing either 16 or 64 molecules, with periodic boundary conditions, was examined using the same ensemble. This latter case can be visualized as representing an extremely large island. Essential to both characterizations is that thermal fluctuations and expansion in the substrate (x,y) plane may proceed in response to changing thermodynamic conditions. The complete monolayer is described by an (N,ρ,T) ensemble with deformable periodic boundary conditions. Although the surface density is constrained to $\rho=1$, consistent with the notion that it is constrained

in plane by the physical and/or grain boundaries, registry is not imposed.

Several order quantities are calculated to assist in interpreting the results. These are

$$O_1=(6N)^{-1}\sum_{i=1}^{N}\left\langle\sum_{s=1}^{6}\exp(i\mathbf{g}_s\cdot\mathbf{r}_i)\right\rangle, \quad (1)$$

$$O_2=\frac{1}{3N(N-1)}\sum_{i<j=1}^{N}\left\langle\sum_{s=1}^{6}\exp(i\mathbf{k}_s\cdot\mathbf{r}_{ij})\right\rangle, \quad (2)$$

$$C(T)=\frac{4}{N(N-1)}\sum_{i<j=1}^{N}\left|\langle(\hat{\mathbf{n}}_i\cdot\hat{\mathbf{n}}_j)^2\rangle-\frac{1}{2}\right|, \quad (3)$$

where the $\mathbf{g}_s$ are reciprocal lattice vectors of the graphite surface, $\mathbf{r}_i$ locates the projection of the ith molecular center onto the surface, and $\mathbf{r}_{ij}=\mathbf{r}_i-\mathbf{r}_j$. The unit vector specifying the orientation of the ith molecules is $\hat{\mathbf{n}}_i$. All vectors are specified with respect to a cartesian reference frame with (x,y) axes on the substrate plane and the origin is at the center of a graphite hexagon. The z axis is normal to the plane. The $\mathbf{k}_s$ are reciprocal lattice vectors of the $\sqrt{3}\times\sqrt{3}$ N_2 lattice. O_1 is designed to equal unity if all N_2 molecular centers are statically situated over the center of a hexagon, and zero if the molecules uniformly sample all (x,y) positions of the graphite surface. Similarly O_2 is unity if N_2 forms a perfect $\sqrt{3}\times\sqrt{3}$ lattice and zero if there is no vestige of this structure. $C(T)$ is unity if N_2 forms a perfect herringbone structure and zero if there are no orientational correlations between molecules, such as for planar free rotor behavior.

Probability distributions $P(X)$ are formed by determining the frequency of occurrence for X in each interval from X to $X+\Delta X$. Each value of X in the distribution represents a bin average over 50 steps.

III. RESULTS

A. Fractional monolayer coverages

Calculations on the 256-molecule patch with free surface boundary conditions, and the $N=16$ and 64 (N,P,T) ensemble with deformable, periodic boundary conditions, both quickly relaxed at the $\sqrt{3}\times\sqrt{3}$ registered phase at low temperatures, and Fig. 1 shows the average surface density of these structures. Registry persists until $T_M\simeq 45$ K, where an abrupt reduction in the density occurs. Above T_M the ensemble with periodic boundary conditions expands to accommodate the new thermodynamic environment. The density is *not* uniform and details will be discussed shortly. The same is true for the patch and we caution that, while they are stable below T_M, they become inherently unstable against disassociation at temperatures sufficiently higher than this. Among the interesting features of this result is the lack of hysteresis. Results starting with a fluidlike configuration and decreasing the temperature through the transition were identical to those proceeding from the solid to the fluid. Also, the remarkably close agreement of results using the two above-mentioned calculational procedures show that the relatively small 256-molecule patch is exhibiting nearly asymptotic behavior. Finally, this figure also shows no size effects. The $N=16$ and 64 (N,P,T) cells give the same results.

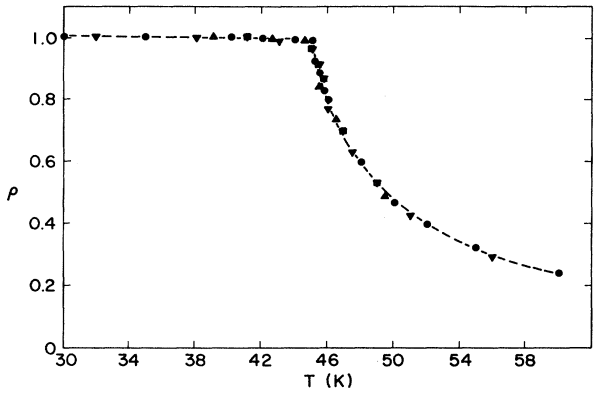

FIG. 1. The triangles show the calculated surface density of the 256-molecule patch, in units of 0.0636 molecules/Å^2. The circles and squares represent results for $N=16$ and 64 molecules in the MC cell, respectively, using an (N,P,T) ensemble. The inverted triangles show results for $N=16$ by cooling from a high-T fluid configuration. The statistical uncertainty in ρ is on the order of ± 0.01.

The internal energy per molecule is shown in Fig. 2, and it also shows an abrupt change in $T\simeq 45$ K. All the features addressed in the above description of Fig. 1 obtain here, except that the finite patch energies are slightly higher than the others, undoubtedly because all bonds are not saturated. The calculated entropy change upon melting, $\Delta S=(\Delta U/T_M)_N=1.76$, is close to the measured value.[8] The specific heat, calculated from the fluctuation theorem, is shown in Fig. 3. Important evidence that the

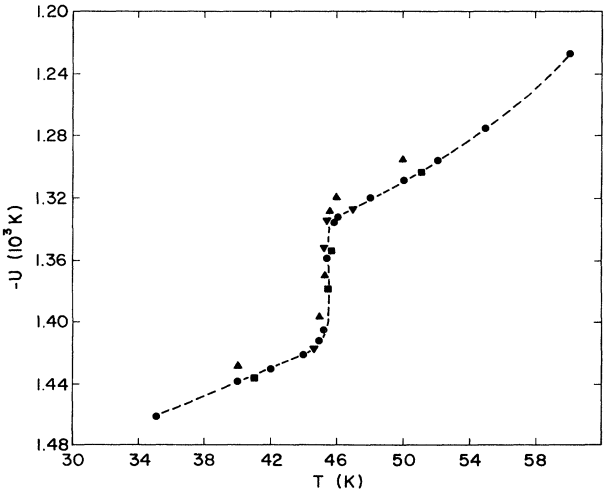

FIG. 2. The internal energy per molecule vs temperature. Format is as in Fig. 1. The dashed line is a fit through the calculated points. The statistical uncertainty is ± 2.5 K, except at the transition, where it is ± 7.0 K.

above-mentioned changes near 45 K signal a melting transition comes from the order parameters shown in Fig. 4. Both O_1 and O_2 rapidly decrease toward zero as the temperature is increased above T_M. In the limit of zero value the former implies all positions above the substrate are equally probable, and the latter indicates there is no vestige of the $\sqrt{3}\times\sqrt{3}$ structure. Note, however, that tails persist in these quantities considerably above T_M, especially in O_1. This indicates that there is some vestige of the $\sqrt{3}\times\sqrt{3}$ order for about 10 K above melting, but even more strong is a modulation of the fluid density around the registry sites at the center of each graphite hexagon. Further evidence of this modulation is given in Fig. 5, where E_1 is the dominant term in Steele's Fourier expansion[29] that accounts for the (x,y) modulation in the substrate interaction. It is designed to be zero if the molecules uniformly sample all positions in the substrate plane and, for N_2, $E_1 \simeq -25$ K for molecules oriented in plane and situated at a registry site. Figure 5 clearly shows an abrupt change at T_M, but it does not go to zero until T is approximately 10 K above melting.

The modulated fluid above melting is more directly noticed by calculating the average density of N_2 molecules across the substrate surface. This is accomplished by identifying small areas $\Delta x\,\Delta y$ across the substrate plane and calculating the frequency of occurrence of N_2 molecular centers in each of these regions. At temperatures $T < T_M$ large, narrow peaks occur at the $\sqrt{3}\times\sqrt{3}$ registry sites, with little or no density in between. Just above the transition much smaller, diffuse peaks occur around each hexagon center (registry site), with considerable density in between. This is the modulated fluid phase. At temperatures greater than 10 K above T_M this feature disappears and the average density is uniform across the surfaces, characteristic of an isotropic fluid. Similar information is reflected in the pair distribution functions, which show sharp peaks at $T < T_M$, characteristic of the $\sqrt{3}\times\sqrt{3}$ separations and, for $T > T_M$, the peaks become much more diffuse and take on the character of a fluid, although a residue of the registered structure is still identifiable for a few degrees above T_M. Again, it must be emphasized that the average density profile across the surface above T_M is much different than it is for each configuration, as will be explained. Finally, monitoring the trajectories of the mass centers for each step along the MC sequences shows small fluctuations about the $\sqrt{3}\times\sqrt{3}$ registry sites at low temperatures, which in-

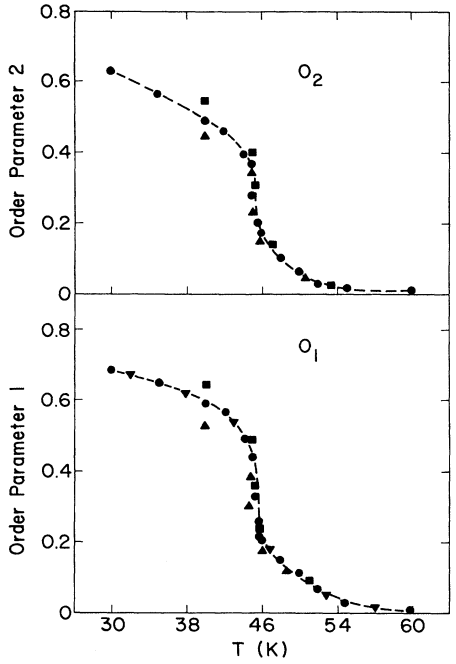

FIG. 4. Calculated translational order parameters O_1 and O_2 vs temperature. Format is as for Fig. 1.

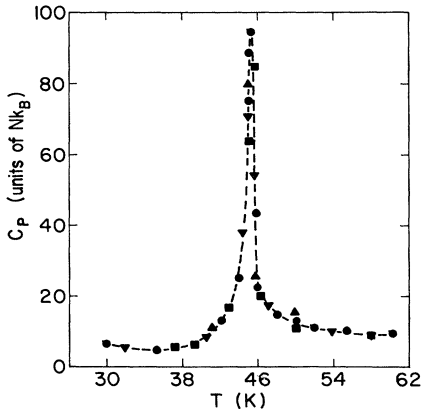

FIG. 3. The specific heat in units of Nk_B, calculated from the fluctuation theorem. Format is the same as Fig. 1. Statistical uncertainties are on the order of ± 1.5, except near the transition, where they are ± 2.5.

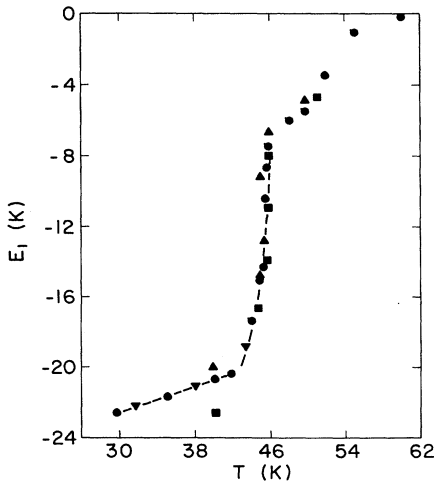

FIG. 5. The lateral contribution to Steele's Fourier expansion of the substrate interaction vs temperature. The format is as in Fig. 1.

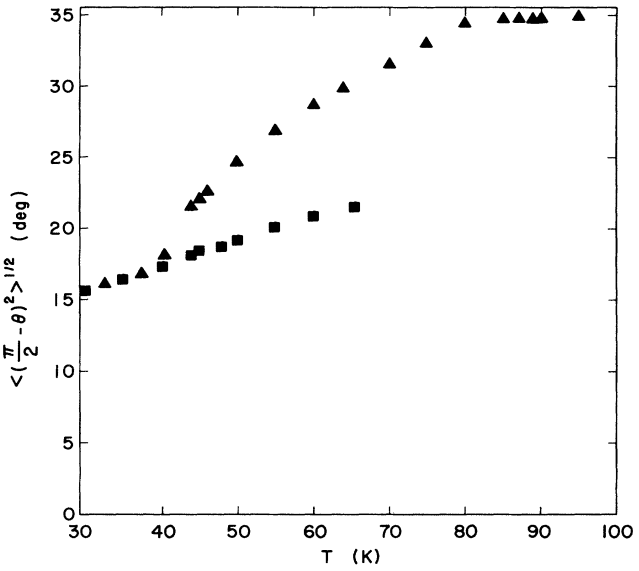

FIG. 6. The calculated root-mean-square orientational fluctuations of the N_2 molecules away from the substrate plane $\langle(\pi/2-\theta)^2\rangle^{1/2}$, vs temperature. The squares represent results for the (N,P,T) ensemble, and the triangles for the $(N,\rho=1,T)$ ensemble.

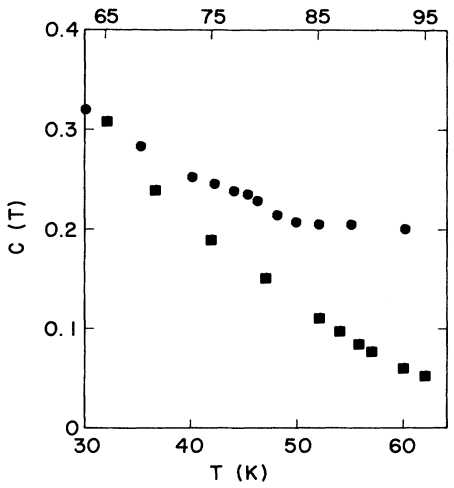

FIG. 7. The circles and squares give the calculated orientational order parameter $C(T)$ for the (N,P,T) and $(N,\rho=1,T)$ ensembles, respectively. The bottom temperature scale refers to the former and the upper the latter. Statistical uncertainty is $|\Delta C|=0.007$.

crease with temperature until T_M, above which they sample all accessible positions, but with a tendency to locate more often in the vicinity of a registry site. This latter feature becomes less apparent as T is increased above T_M. Self-diffusion above T_M is also very pronounced in the 256-molecule patch.

Several calculated quantities expose the orientational characteristics of the N_2 molecules. For all temperatures investigated $30 \leq T \leq 60$ K, the average polar angle $\langle\theta\rangle=\pi/2$, showing that the equilibrium orientation is in the plane of the substrate. However, Fig. 6 shows that the out-of-plane orientational fluctuations $\langle(\pi/2-\theta)^2\rangle^{1/2}$ increase monotonically with temperature, which is also confirmed by the probability distribution $P(\cos\theta)$, that exhibits a peak, symmetric about $\cos\theta=0$, at all temperatures. The peak is very narrow at low temperatures and broadens with increasing T. The distribution $P(\varphi)$ is virtually constant in the azimuthal angle φ, for $30 \leq T \leq 60$ K, indicating a uniform in-plane orientational distribution. The orientational order parameter $C(T)$, shown in Fig. 7, constantly decreases with increasing temperature above the orientational order-disorder transition at $T_{OD} \simeq 27$ K. However, the relatively slow decrease with T above T_{OD} shows that a dynamical vestige of the herringbone structure persists to quite high temperatures. Moreover, the calculated probability distribution $P(\mathbf{n}_i \cdot \mathbf{n}_j)$ at $T=30$ K shows large peaks at $\hat{\mathbf{n}}_i \cdot \hat{\mathbf{n}}_j \pm 1$, and is nearly constant in between, with a weak peak at $\hat{\mathbf{n}}_i \cdot \hat{\mathbf{n}}_j = 0$. These features become less pronounced with increasing T, but there is still some vestige of the peaks at $\hat{\mathbf{n}}_i \cdot \hat{\mathbf{n}}_j = \pm 1$, even at 60 K. This also implies the existence of substantial orientational correlations above melting that could be interpreted as evidence of large intrasublattice correlations and weak intersublattice correlations in the residual herringbone structure.

Table I shows the correlation lengths L_C for $C(T)$ and O_2, which are determined by finding their values for each of the first five nearest-neighbor separations R. These are then fitted to an expression $A \exp(-R/L_C)$. It is evident that the orientational correlations above T_{OD} are very short ranged and decrease monotonically with temperature. Note that they exhibit no signature of partial monolayer melting at $T_M \simeq 45$ K. Also in the same regime, L_C for O_2 decreases monotonically with T in the

TABLE I. The correlation lengths (Å) for the order parameters O_1 and $C(T)$. The upper set of numbers corresponds to the (N,P,T) ensemble for partial monolayers and the lower for $(n,\rho=1,T)$, characterizing the complete monolayer.

T (K)	$L_C(O_2)$	$L_C(C(T))$
30	26.55	3.84
35	23.12	3.43
40	17.66	2.74
45	11.92	2.39
50	7.50	1.98
55	4.97	1.88
60	3.07	1.86
65	25.82	
70	25.22	
75	21.69	
80	21.38	
85	14.75	
90	8.90	
95	4.21	

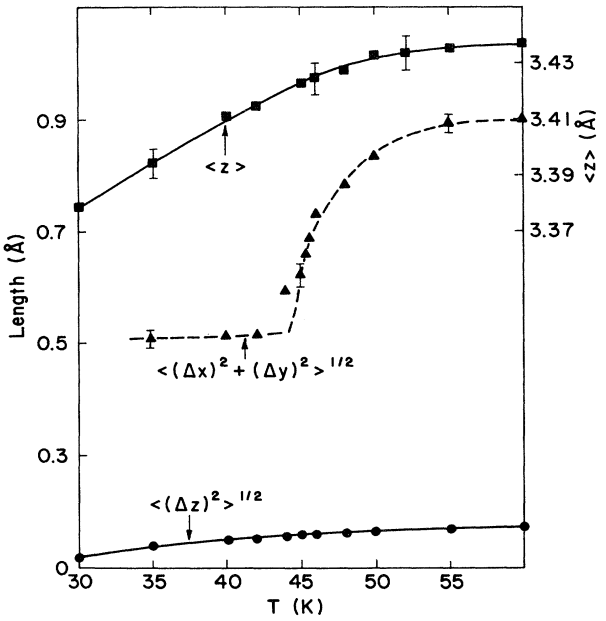

FIG. 8. The circles and triangles are the N_2 mass center fluctuations about their equilibrium positions normal to and parallel to the substrate plane, respectively (left-hand scale). The squares show the average center-of-mass position $\langle z \rangle$ above the substrate plane (right-hand scale). The flags represent typical statistical uncertainties and the lines are fits through the data. Uncertainties in $\langle (\Delta z)^2 \rangle^{1/2}$ are on the order of the data points. Results in this figure are based upon the (N,P,T) ensemble, primarily with $N=16$.

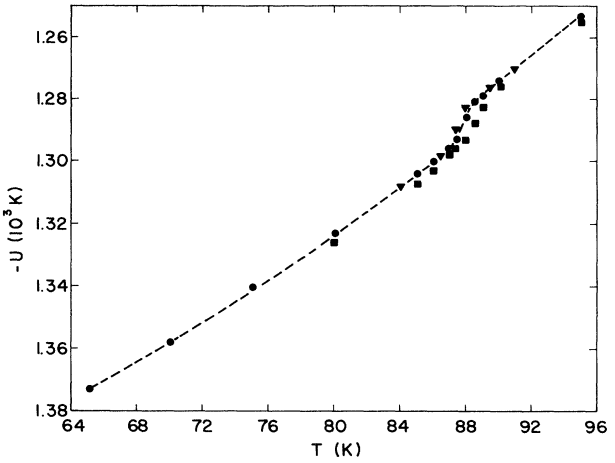

FIG. 9. The circles and squares represent the calculated internal energy per molecule for the $(N,\rho=1,T)$ ensemble, with $N=16$ and 64, respectively. The inverted triangles represent results starting from a fluid initial state at high T and cooling through the transition. The dashed line is a fit through the data points, which have a statistical uncertainty of ± 3.0 K.

range $30 \leq T \leq 60$ K, and shows no signature of the transition.

If our hypothesis for melting of partial monolayers is correct, fluctuations in the (x,y) substrate plane should show a strong signature at melting and fluctuations normal to the plane not. This is clearly the case, as shown in Fig. 8, where $\langle (\Delta x)^2+(\Delta y)^2 \rangle^{1/2}$ dramatically increases at the transition. In-plane fluctuations are taken with respect to the nearest hexagon center (registry point). Note that $\langle (\Delta x)^2+(\Delta y)^2 \rangle^{1/2}=0.917$ Å if the mass centers uniformly sample all points on the substrate surface. Clearly, it is asymptotically approaching this value. Moreover, fluctuations in the $\hat{z}$ direction are small and show no evidence of the transition. Also shown in Fig. 8 is the average position of the molecular centers above the substrate $\langle z \rangle$.

B. The complete monolayer

The complete monolayer has been characterized by an (N,ρ,T) ensemble with $\rho=1$. The calculated energy, shown in Fig. 9, exhibits nominal behavior from $T_{OD} \simeq 27$ K until $T \approx 87$ K, where a clear change occurs. Over this interval the molecules register into the $\sqrt{3}\times\sqrt{3}$ structure. The data points include $N=16$ and 64 cells and hysteresis points. As in the low-temperature transition, there is no noticeable hysteresis, nor are there appreciable size effects. Notice that this transition appears much more gradual than for partial monolayers. The specific heat calculated from the fluctuation theorem is shown in Fig. 10, and the lateral contribution to the substrate interaction energy is shown in Fig. 11. The order parameters O_1 and O_2 are displayed in Fig. 12. They clearly drop sharply toward zero at $T_M \simeq 87$ K. The sharp drop of O_2 to zero indicates that there is little residual $\sqrt{3}\times\sqrt{3}$ order above T_M, as is also evidenced by the sharp drop in its correlation length near melting as shown in Table I. However, the persistence of O_1 to even higher T indicates the existence of a modulated fluid in the region $87 \leq T \lesssim 93$ K. The calculated pair distribution functions, the surface density profiles, and an examination of the mass center trajectories above and below

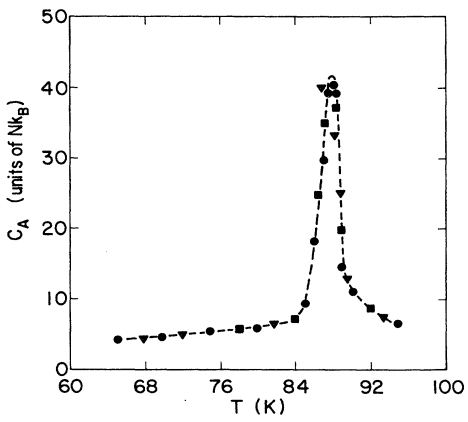

FIG. 10. The calculated specific heat vs T for the $(N,\rho=1,T)$ ensemble. Format is the same as Fig. 9.

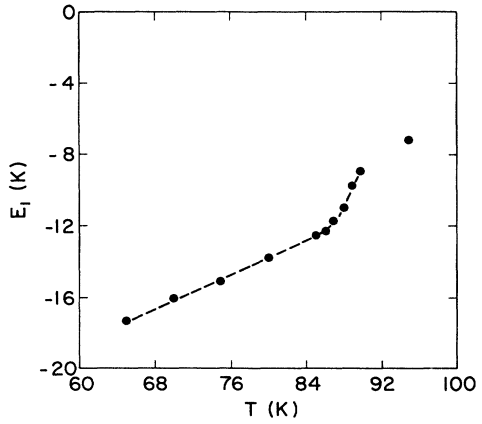

FIG. 11. The solid circles represent the lateral contribution to the substrate energy in Steele's expansion, calculated with the $(N,\rho=1,T)$ ensemble, vs temperature. The dashed line is a fit through the data.

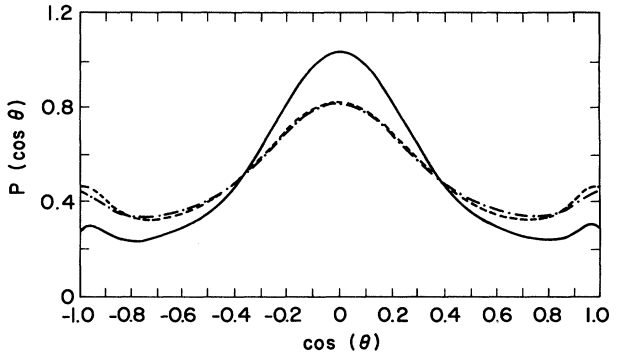

FIG. 13. The solid, dashed, and dot-dashed lines represent the orientational probability distribution $P(\cos\theta)$, vs $\cos\theta$ at temperatures $T=65$, 89, and 95 K, respectively. These are calculated using the $(N,\rho=1,T)$ ensemble.

T_M exhibit features very similar to those described in Sec. III A for the partial monolayer transition, and confirm the modulated fluid regime.

The average orientational angle $\langle\theta\rangle=\pi/2$ over the entire temperature range investigated, $30\leq T\leq 95$ K, but the out-of-plane orientational fluctuations are large, as shown in Fig. 6 for $\langle(\pi/2-\theta)^2\rangle^{1/2}$. This quantity approaches 35° at T_M. There is a distinct difference in $P(\cos\theta)$ from the fractional monolayer case, however. For $T\geq 65$ K there are broad distinct peaks centered about $\cos\theta=0$, but they are superimposed upon a large, nearly uniform background over the range $-1\leq\cos\theta\leq 1$. It is also interesting that wings appear at $\cos\theta\simeq\pm 1$, indicating some propensity for molecules to orient normal to the substrate plane. These features become more pronounced with increasing T. The distributions are shown in Fig. 13 at 65, 89, and 95 K, and are well fit by the polynomial

$$P(\cos\theta)=\sum_{n=0}^{5} a_{2n}(T)P_{2n}(\cos\theta)\ , \tag{4}$$

where the P_{2n} are Legendre polynomials. The coefficients are given in Table II. Over the range $65\leq T\leq 95$ K, the distributions $P(\varphi)$ and $P(\hat{\mathbf{n}}_i\cdot\hat{\mathbf{n}}_j)$ are nearly constant for all arguments, characteristic of a collection of nearly uncorrelated free rotors. The orientational order parameter $C(T)$ is shown in Fig. 7 versus temperature, and demonstrates that herringbone order, while not zero, is rapidly decreasing with increasing temperature.

According to the hypothesis for a complete monolayer, fluctuations in the substrate (x,y) plane should be suppressed and not signal the melting transition, but fluctuations of the N_2 mass centers in the $\hat{\mathbf{z}}$ direction should. It is quite evident from Fig. 14 that this is the case. The fluctuations in the height of the N_2 molecules above the substrate $\langle(\Delta z)^2\rangle^{1/2}$ strongly increase near T_M, and the out-of-plane orientational fluctuations become very large. These are coupled. Note the fluctuations in the substrate plane show no evidence of the transition. Also shown in Fig. 14 is the average mass center position above the substrate $\langle z\rangle$.

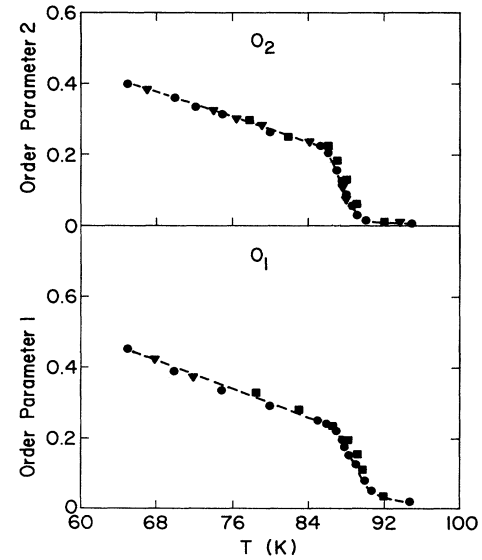

FIG. 12. Calculated translational order parameters O_1 and O_2, calculated using the $(N,\rho=1,T)$ ensemble, vs temperature. Format is the same as for Fig. 9.

TABLE II. Coefficients of the polynomial fit of $P(\cos\theta)$, Eq. (4), for the monolayer at $\rho=1$.

T (K)	a_0	a_2	a_4	a_6	a_8	a_{10}
65	1.0	−0.1959	0.1006	−0.0353	0.0132	−0.0066
85	1.0	−0.1227	0.0737	−0.0222	0.0075	−0.0044
89	1.0	−0.1042	0.0745	−0.0184	0.0055	−0.0051
95	1.0	−0.1064	0.0671	−0.0191	0.0078	−0.0038

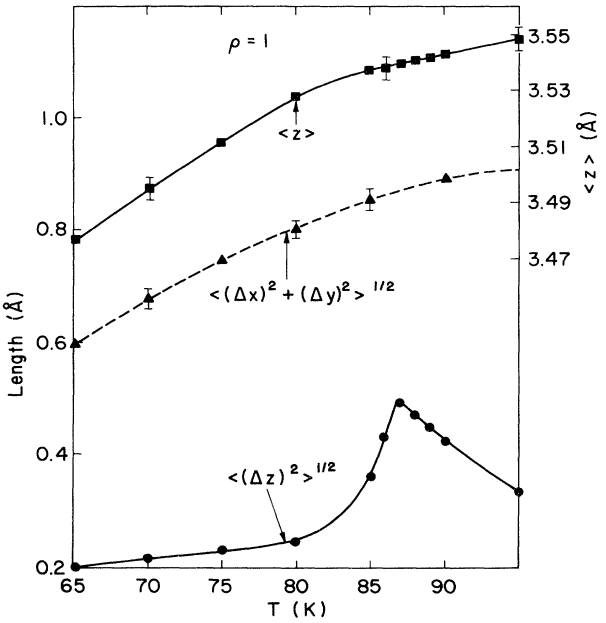

FIG. 14. The center-of-mass fluctuations about equilibrium in the substrate plane and normal to it, and the average mass center positions above the substrate plane $\langle z \rangle$, vs temperature using an $(N,\rho=1,T)$ ensemble. The format is the same as Fig. 8.

IV. CONCLUSIONS

It is evident from this work that differing boundary conditions can have a dramatic influence on predicted properties of N_2 adlayers on graphite, as suggested by the results of Novaco.[32] The notion that in-plane molecular fluctuations and thermal expansion of complete monolayers are constrained by experimental and/or grain boundaries results in a melting temperature higher than for bulk N_2. This is so because out-of-plane translational and orientational fluctuations, required to produce the vacancies necessary to promote melting, are strongly impeded by the large N_2-substrate forces in this direction. This is not the case for partial monolayers, where numerous vacancies exist between islands the relatively weak in-plane forces promote fluctuations and 2D thermal expansion, resulting in much lower melting temperatures. Our calculations of in- and out-of-plane mass center fluctuations, shown in Figs. 8 and 9, support this argument, as do out-of-plane orientational fluctuations. It is evident that this work does not answer all features of 2D melting, but it does provide important insights into the problem and indicates that steric effects are at play. Because the melting curves of many other adlayer systems are very similar to N_2 on graphite, it is imperative to examine whether or not this feature derives from a common root. Some important conclusions of this work are as follows.

(1) The predicted melting temperatures at $T_M=45$ and 87 K for the partial and complete monolayer cases are very close to experimental values.[1,6,8,9]

(2) There is no hysteresis observed in any of the calculations, in that melting and freezing occur at the same temperature.

(3) Melting of the partial monolayer appears as abrupt changes in many physical properties, with an apparent latent heat, as has been argued from experiment.[8,9] The calculated and measured[8] entropy change on transition are in fairly good agreement. There is an apparent lack of hysteresis. As deduced from experiment,[8,9] the complete monolayer melting transition appears gradual.

(4) As established by experiment,[6] the calculated results of all systems studied yield the $\sqrt{3}\times\sqrt{3}$ registered structure for $T<T_M$.

(5) The close agreement between results derived from the 256-molecule cluster with free surface boundary conditions, and the results using an (N,P,T) ensemble, with periodic boundary conditions, shows that island edge effects cannot be a major contributor to melting properties of partial monolayers, except for the aforementioned vacancies separating them.

(6) The prediction of a modulated fluid with local density maxima around registry sites within about 10 K of T_M, for both partial and complete layers, is consistent with previous calculations.[26,28,40] Individual configurations for partial monolayers above T_M, modeled using the (N,P,T) ensemble with periodic boundary conditions, show diffuse islands of molecules along the three equivalent directions of the sixfold graphite symmetry axes, with filamentary threads of molecules between them. These arrangements are very dynamic and lead to the much different average structure defined earlier. The patches with free surface boundary conditions show an even more diffuse nature above T_M, and there is some question about their thermodynamic stability against dissociation. Below T_M they are quite stable and registered.

Just as melting behavior has been deduced by calculating the translational and structural order parameters O_1 and O_2, and by evaluating the pair distribution function and fluctuations in the center of mass degrees of freedom, we utilize order parameters, orientational probability distributions, and fluctuations to determine the orientational behavior of N_2 adlayers on graphite.

In the region $30\leq T\leq 65$ K, calculations using the (N,P,T) ensemble, designed to model fractional monolayer systems, show that the average polar angle of the N_2 molecules in $\langle\theta\rangle=\pi/2$, or in the plane of the substrate, but the out-of-plane fluctuations in this angle increase from 15 to 21° over this interval. The probability distribution $P(\varphi)$ is constant in the azimuthal angle φ and $P(\cos\theta)$ shows relatively sharp peak around $\cos\theta=0$. This is characteristic of a free planar rotor, which appears to be the case, but the molecules also exhibit substantial orientational correlations with their neighbors, at least at the lowest temperatures. The calculated probability distribution $P(\hat{\mathbf{n}}_i\cdot\hat{\mathbf{n}}_j)$ at $T=30$ K has large peaks at $(\hat{\mathbf{n}}_i\cdot\hat{\mathbf{n}}_j)\simeq\pm1$ and is otherwise flat, except for a small, broad peak at zero. The distribution becomes increasingly flat at higher temperatures. Similarly, $C(T)$ though relatively small and decreasing with increasing T, as shown in Fig. 7, still persists above T_{OD}. Thus, the mole-

cules act as planar rotors but also exhibit substantial short-ranged orientational correlations with their neighbors, which become negligible for $T \gtrsim 55$ K.

For the $(N,\rho=1,T)$ ensemble in the interval $45 \leq T \leq 95$ K, which is designed to characterize a complete monolayer, $\langle \theta \rangle = \pi/2$, but out-of-plane fluctuations rise rapidly above 45 K to 35° at 95 K, as shown in Fig. 6. Again, there is no signature of the melting transition at 87 K in either of these quantities. All properties of this system for $T < 45$ K are identical to the already discussed results for the (N,P,T) ensemble. At all $T > T_{OD}$, $P(\varphi)$ is uniform in φ, but $P(\cos\theta)$ shows a distinct evolution with temperature. At low temperatures $P(\cos\theta)$ exhibits a single, well-defined peak about $\cos\theta = 0$, indicating that the molecules are fluctuating about in-plane equilibrium orientations. However, as shown in Fig. (13), the profile broadens considerably with increasing temperature and wings near $\cos\theta = \pm 1$ indicate a propensity for some molecules to orient normal to the plane. There is a point of contact here with previous work,[26,40] performed near 75 K, which showed very similar behavior. Many observations of these works seem reasonable from our results, even though direct comparisons are not possible. Also $P(\hat{\mathbf{n}}_i \cdot \hat{\mathbf{n}}_j)$ is uniform and $C(T)$ drops rapidly toward zero for all $T > 65$ K. Interestingly, the correlation length for O_2 stays relatively constant until near melting, above which it rapidly drops to near zero. Thus, the following picture emerges: The molecules in a complete monolayer act as in-plane 2D rotors with significant short-ranged correlations at temperatures just above T_{OD}, and as nearly free, uncorrelated 3D rotors for $T \gtrsim 95$ K. It is noted that a diffuse embryo of second layer formation begins to appear above melting.

ACKNOWLEDGMENT

This work has been supported by NSF Grant No. DMR-8518453.

[1]R. D. Diehl and S. Fain, J. Chem. Phys. **77**, 5065 (1982).
[2]R. D. Diehl and S. C. Fain, Jr., Surf. Sci. **125**, 116 (1983).
[3]R. D. Diehl, M. F. Toney, and S. C. Fain, Jr., Phys. Rev. Lett. **48**, 177 (1982).
[4]R. D. Diehl and S. C. Fain, Jr., Phys. Rev. B **26**, 4785 (1982).
[5]H. You and S. C. Fain, Jr., Faraday Discuss. Chem. Soc. **80**, 159 (1985).
[6]K. Kjems, L. Passell, H. Taub, J. G. Dash, and A. D. Novaco, Phys. Rev. B **13**, 1446 (1976).
[7]W. Brooks, Brookhaven National Laboratory Report No. 22617, 1977 (unpublished).
[8]M. H. Chan, A. D. Migone, K. D. Miner, and Z. R. Li, Phys. Rev. B **30**, 2681 (1984).
[9]T. Chung and G. Dash, Surf. Sci. **66**, 559 (1977).
[10]A. Inaba and H. Chihara, Can. J. Chem. **66**, 703 (1988).
[11]J. Rouquerol, S. Partyka, and F. Rouquerol, J. Chem. Soc. Faraday Trans. 1 **73**, 306 (1977).
[12]J. Piper, J. Morrison, C. Peters, and Y. Ozaki, J. Chem. Soc. Faraday Trans. **79**, 2863 (1983).
[13]A. D. Migone, H. Kim, M. Chan, J. Talbot, D. Tidesley, and W. A. Steele, Phys. Rev. Lett. **51**, 192 (1983).
[14]J. Kosterlitz and D. Thouless, J. Phys. C **6**, 1181 (1973); B. Halperin and D. Nelson, Phys. Rev. Lett. **41**, 121 (1978); A. Young, Phys. Rev. B **19**, 1855 (1979).
[15]D. Frenkel and J. McTague, Phys. Rev. Lett. **42**, 1632 (1979).
[16]F. Abraham, Phys. Rev. Lett. **44**, 463 (1980).
[17]F. Abraham, Phys. Rev. B **23**, 6145 (1981).
[18]J. Phillips, L. Bruch, and R. Murphy, J. Chem. Phys. **75**, 5097 (1981).
[19]S. Toxvard, Phys. Rev. Lett. **44**, 1002 (1980); **51**, 1971 (1983).
[20]E. Domany and E. Riedel, Phys. Rev. Lett. **40**, 561 (1978).
[21]F. Abraham, Phys. Rev. B **29**, 2606 (1984).
[22]J. A. Combs, Phys. Rev. Lett. **61**, 714 (1988).
[23]W. Brinkman, D. Fisher, and D. Moncton, Science **217**, 693 (1982).
[24]F. Abraham, Phys. Rep. **80**, 339 (1981).
[25]F. Von Swoi, L. Woodcock, and J. Cape, J. Chem. Phys. **73**, 913 (1980).
[26]J. Talbot, D. Tildesley, and W. Steele, Faraday Discuss. Chem. Soc. **80**, 1 (1985).
[27]A. Ostlund and A. Berker, Phys. Rev. Lett. **42**, 843 (1979).
[28]V. Joshi and D. Tildesley, Mol. Phys. **55**, 999 (1985).
[29]W. A. Steele, Surf. Sci. **36**, 317 (1973).
[30]W. Carlos and M. Cole, Surf. Sci. **91**, 339 (1980).
[31]R. D. Etters, M. Roth, and B. Kuchta, Phys. Rev. Lett. **65**, 3140 (1990).
[32]A. Novaco, Phys. Rev. B **35**, 8621 (1987).
[33]R. Berns and A. van der Avoird, J. Chem. Phys. **72**, 6107 (1980).
[34]R. LeSar and R. Gordon, J. Chem. Phys. **84**, 5479 (1986).
[35]R. D. Etters, J. Belak, and R. LeSar, Phys. Rev. B **34**, 4221 (1986); J. Belak, R. D. Etters, and R. LeSar, J. Chem. Phys. **89**, 1625 (1988).
[36]R. D. Etters, V. Chandrsekharan, E. Uzan, and K. Kobashi, Phys. Rev. B **33**, 8615 (1986).
[37]J. Belak, R. LeSar, and R. D. Etters, J. Chem. Phys. **92**, 5430 (1990).
[38]B. Kuchta and R. D. Etters, Phys. Rev. B **36**, 3400 (1987).
[39]B. Kuchta and R. D. Etters, J. Chem. Phys. **88**, 2793 (1987).
[40]A. V. Vernov and William Steele, Langmuir **2**, 219 (1986).